Journal of Materials Chemistry A

Accepted Manuscript

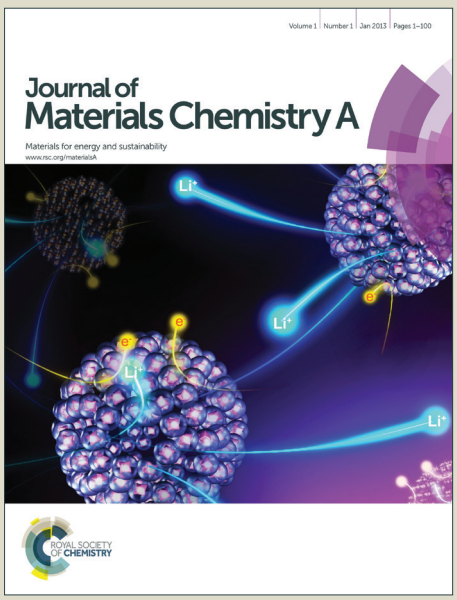

ROYAL SOCIETY OF CHEMISTRY

www.rsc.org/materialsA

Journal Name

RSCPublishing

COMMUNICATION

Infiltrative coating of $LiNi_{0.5}Co_{0.2}Mn_{0.3}O_2$ microspheres with layer-structured $LiTiO_2$: Toward superior cycling performances for Li-ion batteries

Cite this: DOI: 10.1039/xoxxoooooox

Received ooth January 2012,
Accepted ooth January 2012

DOI: 10.1039/xoxxoooooox

www.rsc.org/

Zongyi Wang, Sisi Huang, Baojun Chen, Hao Wu* and Yun Zhang*

Layer-structured $LiTiO_2$ as coating layer is built on the surface of ternary layered $LiNi_{0.5}Co_{0.2}Mn_{0.3}O_2$ microspheres by using a facile infiltrative pre-coating approach. The uniform, nanoscale $LiTiO_2$ coating layer doped with Ni^{2+} and Mn^{4+} ions strongly adheres to the host materials, which endows $LiNi_{0.5}Co_{0.2}Mn_{0.3}O_2$ microspheres with superior high-voltage cycling and thermal stabilities when used as cathode materials for Li-ion battery.

Demands for lithium-ion batteries (LIBs) currently reach from portable electronics to large-scale applications including energy storage systems and electric vehicles.[1] Higher energy density combined with longer cycle life has been one of the key requirements that need to be addressed for these new applications.[2] Layered Li transition metal oxides, $Li[Ni_xCo_yMn_z]O_2$ ($0 \le x,y,z < 1$) (called as LNCM), have served as the mainstream cathode materials toward better LIBs due to their large theoretical capacity (~280 $mAh \cdot g^{-1}$) compared with their olivine- or spinel-structured counterparts.[3] In particular, two variation ternary layered oxides, $LiNi_{1/3}Co_{1/3}Mn_{1/3}O_2$ and $LiNi_{0.5}Co_{0.2}Mn_{0.3}O_2$, have been successfully adopted in commercial LIBs.[4,5] Unfortunately, these materials easily undergo a poor cycling stability if they are charged above 4.2 V at elevated temperatures, due to the dissolution of transition metals from the host structure and decomposition of the organic electrolyte. Surface coating with electrochemically inert oxides and phosphates has been an important approach to strengthen the structural integrity of LNCM materials.[6-9] However, the coating materials are generally unfavourable for both Li^+ ion conduction of cathode materials and interfacial charge transfer of the electrode, giving rise to undesired decline in capacity.[10]

Ternary Li-Ti-O oxide consisting of various stoichiometric and nonstoichiometric compounds has recently received considerable attention because in addition to its application as LIB anode materials with high energy density and rechargeability,[11-16] it also shows a promising role as coating material for surface-modifying electrode materials.[17-20] Monoclinic Li_2TiO_3[17] and spinel $Li_4Ti_5O_{12}$[18,19] have been reported as ideal coating materials being able to ameliorate the electrochemical properties of LNCM materials due to their zero-strain characteristics ensuring high structural stability and fast Li^+ ion mobility. Although the rate capability of LNCM is indeed improved upon coating with these Li-Ti-O oxides, a noticeable capacity decay is still observed when charged at high operating voltage and cycled above room temperature.

Rock salt-type $LiTiO_2$, a layer-structured material, is the end member of a series of compounds, Li_xTiO_2 ($0 \le x \ge 1$), resulting from complete lithium insertion into TiO_2.[21-26] $LiTiO_2$ is believed to possess electronic conductivity because the majority of the Li electrons reside in the Ti-3d/4s hybridised site with ~10% of the electrons being transferred to non localised sites.[22,24] More importantly, $LiTiO_2$ prepared by high-temperature sintering TiO_2 with lithium salt has fully Li-occupied spaces between the octahedra of TiO_2,[25,26] implying $LiTiO_2$ has superior structural stability in organic electrolyte as compared to other Li-Ti-O oxides. In this regard, it is available to establish a thin and complete $LiTiO_2$ coating layer on layered LNCM materials for improving their electrochemical characteristics, especially toward better cycling stability. However, to our best knowledge, there is no report regarding use of $LiTiO_2$ as coating materials for modification of LNCM cathode materials to date.

As to the coating route, traditional approaches such as mechanical mixing and sol−gel methods have been developed,[27-29] but these methods usually suffer from failure in building a uniform, complete, robust and controllable coating layer on the host materials. Specifically, it is difficult with mechanical method to construct a complete coating layer on the host materials, because the coating particles distribute randomly on the surface of the host materials. Moreover, almost all these methods require a post-coating process to produce coating layer under a relatively low temperature, resulting in the weak bonding between the host and the coating layer. Finally, these synthetic routes are often time-consuming and energy-intensive, as a two-step sintering process is generally involved.

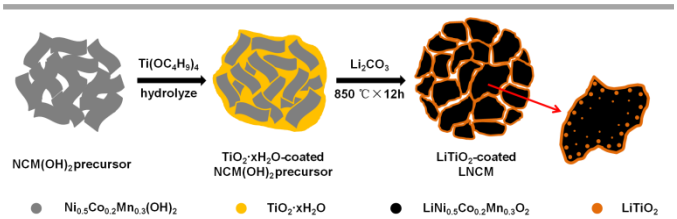

Fig. 1 Schematic illustration of the synthetic route to $LiTiO_2$-coated $LiNi_{0.5}Co_{0.2}Mn_{0.3}O_2$ microspheres

Taking these issues into consideration, herein, we demonstrate a facile infiltrative pre-coating approach, by which a robust, complete, and uniform nanoscale $LiTiO_2$ coating layer doped with Ni^{2+} and Mn^{4+} ions has been achieved on the surface of ternary layered LNCM microspheres (Ni:Co:Mn = 5:2:3 in molar ratio). The synthetic strategy of the coated LNCM consists of two steps, in which mesoporous $Ni_{0.5}Co_{0.2}Mn_{0.3}(OH)_2$ microspheres were first surface-modified by a $TiO_2{\cdot}xH_2O$ pre-coating process, followed by lithiation of the coated microspheres by a single-step sintering to give the final $LiTiO_2$-coated LNCM products (Fig. 1).

Ni-rich mesoporous $Ni_{0.5}Co_{0.2}Mn_{0.3}(OH)_2$ microspheres, obtained by a co-precipitation method, were chosen as the precursors, not only due to their three-dimensional spherical architecture, but also because of the porous structure of continuous mesorpores, as proved by N_2 adsorption–desorption analysis (Fig S1, ESI†). The porous structure is benefit to subsequent inside-out infiltration of $Ti(OC_4H_9)_4$ throughout the entire microspheres,[30] where $Ti(OC_4H_9)_4$ first enters into the void spaces by capillary action, and then disperses on the surface of the microspheres. After slowly hydrolyzing $Ti(OC_4H_9)_4$, an uniform nanoscale $TiO_2{\cdot}xH_2O$ pre-coating layer was formed within the pores and on the surface of the microspheres, which is confirmed by the decreased pore size and increased BET surface area of the coated microspheres (Table S1, ESI†). Two products of $LiTiO_2$-coated LNCM with Ti:(Ni+Co+Mn) = 1 and 5% in molar ratio were subsequently obtained from sintering at 850 ℃ with Li_2CO_3.

All the prepared materials including precursors, $TiO_2{\cdot}xH_2O$-coated precursors and $LiTiO_2$-coated LNCM exhibit micronsized spherical morphology under SEM observations in Fig. S2 (ESI†) and Fig. 2. Fig. S2(a) and 2(b) shows that uniform and monodispersed precursor microspheres with rough surface are composed of cross-stacked flake-like primary particles with about 500~800 nm in width and 1.5~3 μm in length. The unique spherical shape of the precursor particles is well inherited after hydrolyzing formation of an additional amorphous coating layer of $TiO_2{\cdot}xH_2O$ around the core particles, as shown in Fig. 2(a) and 2(b). In comparison with the 1 mol% coated precursor, the microspheres in 5 mol% one have more dense and smooth surface owing to higher TiO_2 coating content. After sintering with lithium salt, the coated microspheres underwent an expansion in the bulk due to the insertion of lithium, but the size of every flaked primary particle contrarily decreased to be 200 ~ 300 nm in width and 400~700 nm in length. Also, a thin coating layer is clearly discerned the surface of the microspheres, as shown in Fig. 2(c) and 2(d). XRD patterns indicate that both the two products match with identical hexagonal α-$NaFeO_2$ layered structure with clear (006) and (012) peaks around 38 °(Fig S3a, ESI†),[31] and there is no change in the crystalline structure of LNCM after coating. It should be noted that no peaks corresponding to rock salt-type $LiTiO_2$ could be found, due to the low loading content and possible diffusion of Ti ions from surface into the bulk of host LNCM materials.[17] As shown in Table S2 (ESI†), the calculated lattice parameters and unit cell volumes of the 1 and 5 mol% coated LNCM became larger with the increase of $LiTiO_2$ content, suggesting that Ti^{3+} ions would infiltrate from the surface into the layered host structure as doping ions due to the fact that the ionic radius of Ti^{3+} (76 pm) is larger than that of Mn^{4+} (67 pm).[37,38] However, two characteristic diffraction peaks, indexed to the (200) and (220) planes of rock salt-type $LiTiO_2$ (JCPDS No. 74-2257, Fig S3b, ESI†),[21,23] appear around 43.8 ° and 63.7 ° by further increasing the Ti:(Ni+Co+Mn) content to 10 mol%. This demonstrates that $LiTiO_2$ is indeed formed and present on the surface of LNCM under our synthetic conditions.

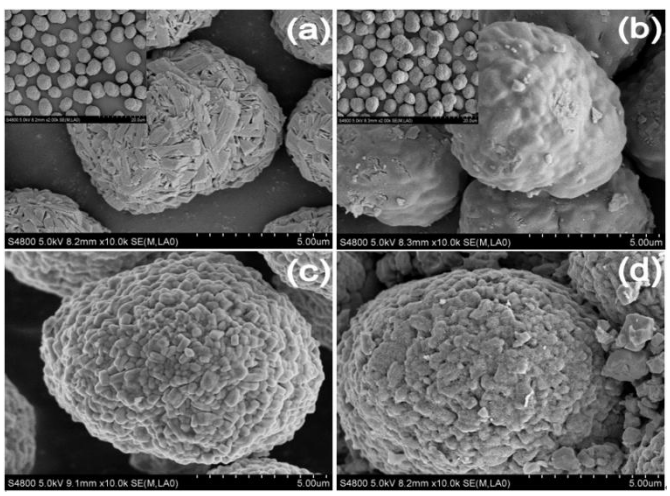

Fig. 2 SEM images of (a and b) $TiO_2{\cdot}xH_2O$-coated $Ni_{0.5}Co_{0.2}Mn_{0.3}(OH)_2$ and (c and d) $LiTiO_2$-coated LNCM. The content of Ti: (a and c) 1% and (b and d) 5%; Insets in (a) and (b) show the SEM images at low magnification.

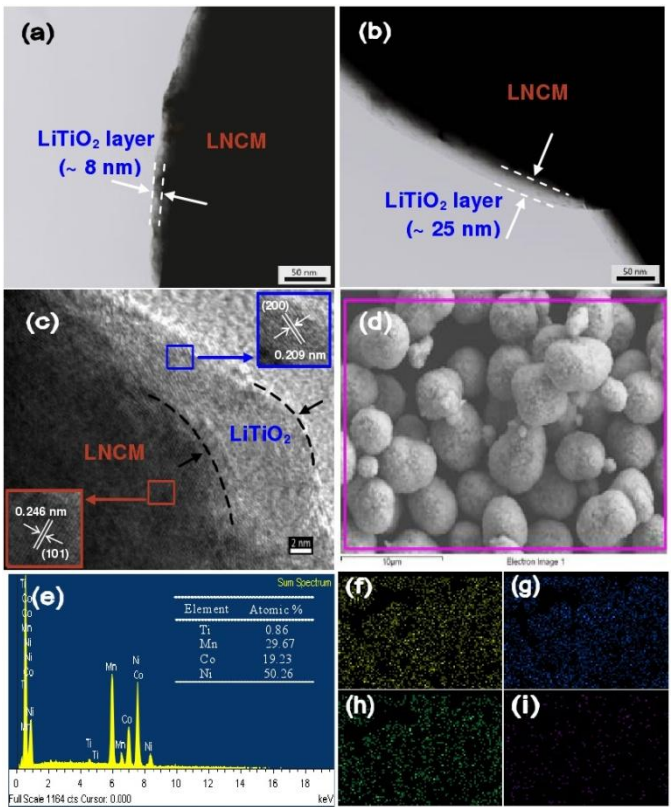

Fig. 3 TEM images of (a) 1 mol% and (b) 5 mol% $LiTiO_2$-coated LNCM. (c) HRTEM image of 1 mol% $LiTiO_2$-coated LNCM; Inserts show the lattice fringes from selected square regions. (d) SEM image and (e) EDS spectrum of 1 mol% $LiTiO_2$-coated LNCM. (f–i) EDS dot-mapping results of Mn (f), Co (g), Ni (h), and Ti (i).

The typical TEM images are presented in Fig. 3(a) and 3(b), in which a thin and complete coating layer is obviously seen on the surface of LNCM particles, and its thickness increases with increasing TiO_2 amount. Further observation into the 1 mol% product by high-resolution TEM (HRTEM) reveals that there is a boundary between the core and shell material, and the outer layer with a thin thickness of ~8 nm is covered on the surface of core particle (Fig. 3(c)). The lattice spacing of ~0.246 nm in the core

particle marked by orange colour is in good agreement with the *d*-spacing of (101) plane of LNCM,[32] while the interplanar distances in the marked blue region taken from the outer layer is estimated to be ~0.209 nm, which is ascribed to the (200) plane of rock salt-type $LiTiO_2$.[23] EDS analysis (Fig. 3(e)) indicates that the 1 mol% product has an atomic ratio of 0.0086Ti, 0.5Ni, 0.19Co, and 0.29Mn, which is nearly consistent with the initially designed composition. EDS dot-mapping for Mn, Co, Ni, and Ti in Fig 3(f)-3(c) further reveals that these elements homogeneously distribute in the selected region of 1 mol% product (Fig 3d), indicating that the obtained materials were uniformly coated. XPS was used to determine the surface content of elements in the two products, and the results are presented in Fig S5 (ESI†). By XPS characterization, the valences are determined to be 2+, 3+, 4+, and 3+ for Ni, Co, Mn, and Ti, respectively.[33] Based on the elemental quantification analysis of XPS, the surface contents of Ni^{2+} and Mn^{4+} ions which are higher than the bulk values indicate the doping of Ni^{2+} and Mn^{4+} ions into the surface $LiTiO_2$ coating layer (Table S3, ESI†).[17] Accordingly, the coated LNCM microspheres are described as surface-$LiTiO_2$-rich microspheres, with $Li[Ni_xMn_yTi_{1-x-y}]O_2$ domains in the surface layer. This unique coating layer indicates a strong interaction between $LiTiO_2$ and the host structure, giving rise to more excellent structural stability than traditional coating layers, as well as superior long-term cycling capability.

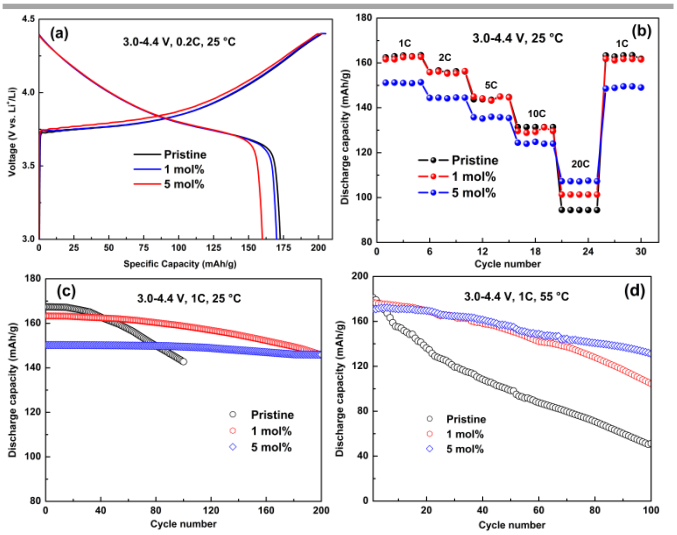

Fig. 4 (a) Initial charge and discharge curves of pristine and coated LNCM microspheres under a current rate of 0.2 C. (b) Rate capability under variable current rate. (c and d) Cycling performance at 25 and 55 ℃ under a current rate of 1C. All measurement were conducted in the voltage range of 3.0–4.4 V vs. Li/Li^+.

The electrochemical performances of the coin-type cells with as-prepared $LiTiO_2$-coated LNCM microspheres and pristine counterpart as cathode materials were evaluated. Fig. 4a shows the typical initial charge/discharge curves of the cells under a current rate of 0.2 C (1 C = 150 mA/g) in the voltage range of 3.0–4.4 V at 25 ℃. The charge/discharge curves of all the cells are smooth with a monotonous voltage plateau, while the discharging average voltage slightly changed after 1 mol% $LiTiO_2$ coating. The 1 mol% coated LNCM exhibits a discharge capacity of 170 mAh/g, which is close to that of 172 mAh/g for the pristine one. $LiTiO_2$ is electrochemically inactive within these voltage ranges, and coating amount higher than 1 mol% leads to obvious polarization and capacity loss, presumably due to increased contact resistance and charge transfer resistance.[34] Fig. 4b compares the rate performances of cells evaluated at variable current rates of 1~10 C for 5 cycles at each current rate. It is observed that the capacities of all the cells decreased as cycling current rate increased (Fig. S6 and Table S4, EIS†), which is caused by the low diffusion rate of the Li^+ ions into/off electrodes at high rates.[34] The 1 mol% coated LNCM can be reversibly cycled at 1, 2, 5 and 10 C with stable discharge capacities of 163, 155, 144 and 130 mA h/g, respectively, which is nearly as good as the uncoated electrode. However, the rate capability sharply decreased for coating amounts higher than 1 mol%; the 5 mo% coated LNCM exhibits a remarkable decline in capacity at every current rate as compared to the pristine one, because severe polarization might occur within the electrode upon coating with excess $LiTiO_2$. Although $LiTiO_2$ has been regarded as an electronic conductor, occupation of all available sites upon Li-insertion into TiO_2 leads to significant reduction of the Li-diffusion in $LiTiO_2$,[24] and thus the poor Li^+ ionic conductivity limits the contribution of $LiTiO_2$ on the improvement of rate performance of LNCM in present study. Nevertheless, it should be noted that the discharge capacities of coated LNCM at higher current rate of 20 C are obviously higher than that of pristine counterpart (Table S4, EIS†), indicating that the high-rate capability of LNCM can be indeed improved upon $LiTiO_2$ coating. In addition, the capacities of all the cells returned to almost the original values when the current rate was finally reduced back to 1 C, suggesting the good reversibility of the as-prepared cathode materials.

Despite the indistinctive amelioration in rate capability of LNCM with $LiTiO_2$ coating, the long-term cycling tests demonstrate that the coated LNCM has remarkably improved high-voltage cycling stability than the pristine counterpart (Fig. S7 and Table S5, EIS†). A new batch of cells was subjected to cycle under 1 C in operating voltage of 3.0–4.4 V at 25 ℃, and the test results are displayed in Fig. 4c. Clearly, the uncoated electrode suffered from a severe capacity fading during the cycles, whereas only 3.6% capacity decay was observed for 1 mol% coated LNCM in the first 100 cycles, and the reversible capacity of 145 mAh/g (89% retention) was still retained after subsequent 100 cycles. Better capacity retention can be achieved in 5 mol% coated electrode which delivered the capacity retention as high as 97% even at the end of 200 charge/discharge cycles. EIS was performed on the cells after 100 cycles to reveal the origin of the improved cycling performance of the coated LNCM (Fig S8, ESI†). The Nyquist plots of all materials observe the same equivalent circuit. In particular, the increases in charge transfer resistances (R_{ct}) for the coated LNCM electrodes after 100 cycles are much smaller than that for the uncoated electrode (Table S6, ESI†). This observation indicates that $LiTiO_2$ functions as a protective layer to cover the active cathode sites and reduce the oxidative decomposition of the electrolyte at high voltage, such that the structural stability of cathode material can be enhanced.[35] Fig S9 (ESI†) presents the SEM image and EDS spectrum of the 5 mol% coated LNCM electrode after 100 cycles. It can be seen from Fig S9a and 9b (ESI†) that after 100 cycles, the coated LNCM still maintains original spherical morphology and the rougher surface is indicative of forming a thin SEI film. EDS analysis (Fig S9c and 9d, ESI†) also reveals that there is nearly no change in the chemical composition of the electrode material in addition to a small amount of phosphorus detected. Accordingly, the excellent cycling performance of the modified LNCM cathode material is attributed to its enhanced structure stability upon the $LiTiO_2$ coating.

Coated LNCM also exhibit more inspiring thermal stability than the pristine counterpart when cycling at 55 ℃ (Fig. 4d). At 55 ℃, the pristine, 1, and 5 mol% $LiTiO_2$-coated LNCM cathode materials delivered initial discharge capacities of 181, 177, and 170 mAh/g, respectively, which are higher than those obtained at 25 ℃ (Table S5, ESI†). After 100 consecutive cycles, the 1 and 5 mol% coated LNCM can still deliver outstanding capacity retention of 60 and 77% respectively, much higher than that of 28% for the pristine counterpart. This is ascribed to that the uniform, complete and robust

coating layer of $LiTiO_2$ renders the LNCM materials more resistive against the attack of HF produced from the electrolyte decomposition at high temperature.[36] In addition, doping of Ni^{2+} and Mn^{4+} ions into the surface layer also helps to consolidate the interfacial interaction between coating layer and host structures. Due to this reason, the $LiTiO_2$-coated microspheres could be capable for cycling under higher working voltage and elevated temperature, which will increase the capacity that material deliver.

Conclusions

In summary, we have successfully demonstrated coating of LNCM microspheres with layer-structured rock salt-type $LiTiO_2$ by using a facile and versatile coating approach based on infiltrative pre-coating a $TiO_2{\cdot}xH_2O$ layer on mesoporous $Ni_{0.5}Co_{0.2}Mn_{0.3}(OH)_2$ microspheres as precursors, followed by a single-step sintering process. The electrochemical performances of the pristine and $LiTiO_2$-coated LNCM as cathode materials at a cutoff potential of 4.4 V were compared at 25 and 55 ℃. Although $LiTiO_2$ coating indistinctively improved the rate capability, the 1 and 5 mol% coated LNCM exhibited inspiring high-voltage cycling capability as well as thermal stability than the pristine counterpart. Such impressive cycling performances are attributed to the robust structure feature of $LiTiO_2$ protective layer and the strengthened interfacial stability between coating layer and host LNCM material derived from the facile and versatile coating approach. The present work indicates that the layer-structured rock salt-type $LiTiO_2$ can be used as the suitable candidate of coating materials toward developing higher energy density electrode materials together with longer cycle life for LIBs.

The authors acknowledge the financial support from National Basic Research Program of China (973 program no. 2013CB934700) and the Sichuan Province Science and Technology Support Program (no. 2014GZ0093).

Notes and references

Address: College of Materials Science and Engineering, Sichuan University, Chengdu 610064, China.
E-mail: hao.wu@scu.edu.cn and y_zhang@scu.edu.cn

†Electronic Supplementary Information (ESI) available: [Experimental and characterization details; Fig S1-S9 and Table S1-S6]. See DOI: 10.1039/c000000x/

1 J. M. Tarascon and M. Armand, *Nature*, 2001, **414**, 359-367.
2 K. Kang, Y. S. Meng, J. Breger, C. P. Grey and G. Ceder, *Science*, 2006, **311**, 977-980.
3 T. Ohzuku and Y. Makimura, *Chem. Lett.*, 2001, **30**, 642-643.
4 L. Wang, J. Li, X. He, W. Pu, C. Wan and C. Jiang, *J. Solid State Electrochem.*, 2009, **13**, 1157-1164.
5 Y. K. Sun, S. T. Myung, M. H. Kim, J. Prakash and K. Amine, *J. Am. Chem. Soc.*, 2005, **127**, 13411–13418.
6 J. Cho, Y. J. Kim, T. J. Kim and B. Park, *Angew. Chem., Int. Ed.*, 2001, **40**, 3367.
7 M. M. Thackeray, C. S. Johnson, J. S. Kim, K. C. Lauzze, J. T. Vaughey, N. Dietz, D. Abraham, S. A. Hackney, W. Zeltner and M. A. Anderson, *Electrochem. Commun.*, 2003, **5**, 752-758.
8 C. Li, H. P. Zhang, L. J. Fu, H. Liu, Y. P. Wu, E. Rahm, R. Holze and H. Q. Wu, *Electrochim. Acta*, 2006, **51**, 3872-3883.
9 S. Lim and J. Cho, *Chem. Commun.*, 2008, 4472-4474.
10 J. H. Park, J. H. Cho, S. B. Kim, W.S. Kim, S. Y. Lee and S. Y. Lee, *J. Mater. Chem.*, 2012, **22**, 12574-12581.
11 L. Yu, H. B. Wu and X. W. Lou, *Adv. Mater.*, 2013, **25**, 2296-2300.
12 W. N. Chen, H. Jiang, Y. J. Hu, Y. H. Dai and C. Z. Li, *Chem. Commun.*, 2014, **50**, 8856-8859.
13 L. Persi, F. Croce and B. Scrosati, *Electrochem. Commun.*, 2002, **4**, 92-95.
14 J. W. Yang, J. Zhao, Y. Z. Chen and Y. W. Li, *Ionics*, 2010, **16**, 425-429.
15 C. S. Johnson, J. S. Kim, A. J. Kropf, A. J. Kahaian, J. T. Vaughey and M. M. Thackeray, *J. Power Sources*, 2003, **119**, 139-144.
16 M. Vijayakumar, G. Hirankumar, M.S. Bhuvaneswari and S. Selvasekarapandian, *J. Power Sources*, 2003, **117**, 143-147.
17 J. Lu, Q. Peng, W. Y. Wang, C. Y. Nan, L. H. Li and Y. D. Li, *J. Am. Chem. Soc.*, 2013, **135**, 1649-1652.
18 Y. R. Zhu, T. F. Yi, R. S. Zhu and A. N. Zhou, *Ceram. Int.*, 2013, **39**, 3087-3094.
19 Y. J. Liu, Y. Y. Gao, Q. L. Wang and A. C. Dou, *Ionics*, 2014, **20**, 739-745.
20 Y. P. Tang, X. X. Tan, G. Y. Hou and G. Q. Zheng, *Electrochim. Acta*, 2014, **117**, 172-178.
21 K. Jiang, X. H. Hu, H. J. Sun, D. H. Wang, X. B. Jin, Y .Y . Ren and G. Z. Chen, *Chem. Mater.*, 2004, **16**, 4324-4329.
22 W. C. Mackrodt, *J. Solid State Chem.*, 1999, **142**, 428-439.
23 X. R. Pei, S. L. Zhang, J. W. Zhang, J. J. Yang and Z. S. Jin, *J. Inorg. Mater.*, 2007, **22**, 84-88.
24 W. J. H. Borghols, D. Lutzenkirchen-Hecht, U. Haake, E. R. H. van Eck, F. M. Mulder and M. Wagemaker, *Phys. Chem. Chem. Phys.*, 2009, **11**, 5742-5748.
25 L. Benco, J. L. Barras and C. A. Daul, *Inorg. Chem.*, 1999, **38**, 20-28.
26 B. J. Morgan, *J. Phys. Chem. Lett.*, 2011, **2**, 1657-1661.
27 C. Li, H. P. Zhang, L. J. Fu, H. Liu, Y. P. Wu, E. Ram, R. Holze and H. Q. Wu, *Electrochim. Acta*, 2006, **51**, 3872-3883.
28 L. J. Fu, H. Liu, C. Li, Y. P. Wu, E. Rahm, R. Holze and H. Q. Wu, *Solid State Sci.*, 2006, **8**, 113-128.
29 J. P. Zhao and Y. Wang, *J. Phys. Chem. C*, 2012, **116**, 11867-11872.
30 H. G. Jung, S. T. Myung, C. S. Yoon, S. B. Son, K. H. Oh, K. Amine, B. Scrosati and Y. K. Sun, *Energy Environ. Sci.*, 2011, **4**, 1345-1351.
31 N. N. Sinha and N. Munichandraiah, *J. Electrochem. Soc.*, 2010, **157**, A647-A653.
32 S. K. Jung, H. Gwon, J. Hong, K. Y. Park, D. H. Seo, H. Kim, J. Hyun, W. Yang and K. Kang, *Adv. Energy Mater.*, 2014, **4**, 1300787.
33 C. D. Wagner and G. E. Muilenberg, *Handbook of x-ray photoelectron spectroscopy: a reference book of standard data for use in x-ray photoelectron spectroscopy*, Perkin-Elmer Corp., Physical Electronics Division: 1979.
34 K. Yang, L. Z. Fan, J. Guo and X. H. Qu, *Electrochim. Acta*, 2012, **63**, 363-368.
35 S. H. Ju, I. S. Kang, Y. S. Lee, W. K. Shin, S. Kim, K. Shin and D. W. Kim, *ACS Appl. Mater. Interfaces*, 2014, **6**, 2546-2552.
36 S. U. Woo, B. C. Park, C. S. Yoon, S. T. Myung, J. Prakash and Y. K. Sun, *J. Electrochem. Soc.*, 2007, **154**, A649-A655.
37 X. K. Yang, R. Z. Yu, L. Ge, D. Wang, Q. L. Zhao, X. Y. Wang, Y. S. Bai, H. Yuan and H. B. Su, *J. Mater. Chem. A*, 2014, **2**, 8362-8368.
38 M. Lin, S. H. Wang, Z. L. Gong, X. K. Huang and Y. Yang, *J. Electrochem. Soc.*, 2013, **160**, A3036-A3040.

